Vision Research 165 (2019) 13–21

Contents lists available at ScienceDirect

Vision Research

journal homepage: www.elsevier.com/locate/visres

Spatial frequency selectivity of the human visual cortex estimated with pseudo-random visual evoked cortical potential (VECP)

Isabelle Christine V.S. Martins[a,d], Alódia Brasil[b,d], Letícia Miquilini[a,c,d], Paulo Roney Kilpp Goulart[c,d], Anderson Manoel Herculano[a,d], Luiz Carlos L. Silveira[a,b,c,d,1], Givago S. Souza[a,b,d,*]

[a] Instituto de Ciências Biológicas, Universidade Federal do Pará, Belém, Pará, Brazil
[b] Núcleo de Medicina Tropical, Universidade Federal do Pará, Belém, Pará, Brazil
[c] Núcleo de Teoria e Pesquisa do Comportamento, Universidade Federal do Pará, Brazil
[d] Universidade do Ceuma, São Luís, Maranhão, Brazil

ARTICLE INFO

Keywords:
Color vision
Spatial selectivity
Human visual cortex
Visual evoked potential

ABSTRACT

Single-cell recordings in the primary visual cortex (V1) show neurons with spatial frequency (SF) tuning, which had different responses to chromatic and luminance stimuli. Visually evoked cortical potential (VECP) investigations have reported different spatial profiles. The current study aimed to investigate the spatial selectivity of V1 to simultaneous stimulus of chromatic and luminance contrasts. Compound stimuli temporally driven by m-sequences at 8 SFs were utilized to generate VECP records from thirty subjects (14 trichromats and 16 colorblind subjects). We extracted the second-order kernel, first and second slices (K2.1 and K2.2, respectively). Optimal SF, SF bandwidth, and high SF cut-off were estimated from the best-fitted functions to the VECP amplitude vs SF. For trichromats, K2.1 waveforms had a negative component (N1 K2.1) at 100 ms followed by a positive component (P1 K2.1). K2.2 waveforms also had a negative component (N1 K2.2) at 100 ms followed by a positive deflection (P1 K2.2). SF tuning of N1 K2.1 and N1 K2.2 had a band-pass profile, while the P1 K2.1 was low-pass tuned. P1 K2.1 optimal SF differed significantly from both other negative responses and from P1 K2.2. We found differences in the optimal SF, SF tuning and high SF cut-off among the VECP components. Dichromats had little or no response for all stimulus conditions. The absence of the responses in dichromats, the similarity between the high SF cut-off of the pseudorandom VECPs and psychophysical chromatic visual acuity, and presence of multiple SF tunings suggested that pseudorandom VECPs represented the activity of cells that responded preferentially to the chromatic component of the compound stimuli.

1. Introduction

Lee, Sun, and Valberg (2011) introduced a new stimulus which was simultaneously composed of chromatic and luminance contrast. This stimulus compound stimulus featured a luminance component with doubled spatial and temporal frequencies compared with the chromatic component of the stimulus. The authors have observed that primate retinal ganglion P cells respond to the compound stimulus mainly in the first harmonic (temporal frequency = 1.6 Hz), while the responses of primate ganglion M cells have reliable response to the first and the second harmonic (temporal frequency of the first harmonic = 2 Hz, temporal frequency of the second harmonic = 4 Hz). Ganglion P cells responses to compound stimulus and chromatic stimulus were similar, while for ganglion M cells the similarity between responses occurred for compound and luminance stimuli.

Later, Parry et al. (2012) investigated temporal tuning of the full-field electroretinogram elicited by a compound stimulus. They found that for trichromats, the first harmonic showed low-pass temporal tuning such as expected for color-opponent cells like P cells, while the second harmonic had a band-pass temporal tuning such as expected for luminance-opponent cells like M cells. Dichromats had low amplitude in the first harmonic and normal second harmonic with the same temporal tuning of the trichromats. Li et al. (2014) used a compound stimulus to elicit responses from primate primary visual cortex cells. They described cells with prominent responses to the chromatic component of the compound stimulus and cells that responded mainly to

* Corresponding author at: Universidade Federal do Pará, Núcleo de Medicina Tropical, Av. Generalíssimo Deodoro 92 (Umarizal), 66055-240 Belém, Pará, Brazil.
E-mail address: givagosouza@ufpa.br (G.S. Souza).
[1] Deceased.

https://doi.org/10.1016/j.visres.2019.09.004
Received 8 December 2018; Received in revised form 20 June 2019; Accepted 18 September 2019

the luminance component of the compound stimulus. Additionally, they observed that some cells responded for the chromatic component (first harmonic) and for the luminance component (second harmonic) of the compound stimulus. They suggested that the primary visual cortex possibly combines signals from P and M pathway to increase the receptive field diversity and optimize the visual processing of scenes mixing chromatic and luminance information. Lee et al. (2011) and Cooper, Sun, and Lee (2012) estimated the contrast sensitivity functions for different types of compound stimuli and compared to the contrast sensitivity estimated from a stimulus with isolated luminance contrast and chromatic contrast. They observed that the measurements estimated with the compound stimulus followed the more sensitive mechanism (luminance or color) in that specific spatial frequency (SF).

In the primary visual cortex (V1) of primates, there are controversies regarding the processing of color contrast information (Johnson, Hawken, & Shapley, 2001). Some studies have shown that in V1, there are few cells responsive to purely chromatic stimuli (Hubel & Wiesel, 1968; Lennie, Krauskopf, & Sclar, 1990), while other studies have found a reasonable number of color responsive cells (Dow, 1974; Johnson et al., 2001; Thorell, De Valois, & Albrech, 1984). Johnson et al. (2001) found, in *Macaca fascicularis*, that some cells showed little or no response to equiluminant stimuli, but they responded well to luminance. Other cells showed comparable responses to isoluminant and luminance gratings. Other cellular groups had robust responses to equiluminant gratings and little or no response to luminance gratings.

Another point of controversy in the functional reports about color vision on different levels of visual system processing is the spatial selectivity for chromatic stimulation. For cellular recordings in V1 of non-human primates, Thorell et al. (1984) found band-pass tuning for most of the cortical cells, especially those with double opponency for color. Lennie et al. (1990) also found band-pass spatial selectivity for the red-green color axis. Johnson et al. (2001) showed that V1 cells that responded only to the equiluminant color stimulus had low-pass tuning, while those responsive cells for color and luminance stimuli had band-pass tuning, as well as cells responsive only to the luminance contrast. This discussion about the different mechanism of spatial selectivity for color stimulus is also evident in psychophysical studies, as shown in several investigations (Mullen, 1985; Vimal, 1998, 2002; Webster, De Valois, & Switkes, 1990). Mullen (1985) estimated the psychophysical chromatic contrast sensitivity function in humans. The chromatic contrast sensitivity functions for red-green and blue-yellow mechanisms had spatial low-pass tuning, while for luminance contrast, the contrast sensitivity as a function of the SF was band-pass tuned. Other studies used adaptation or masking methods to study the basic mechanisms responsible for the generation of the spatial chromatic contrast sensitivity function. They used a model of multiple mechanisms, and they found that 6 different mechanisms, namely, C1, C2, C3, C4, C5, and C6, composed the chromatic contrast sensitivity function. They observed that C1 had spatial low-pass tuning while all the other mechanisms were featured by spatial band-pass functions, peaking at 0.13 cpd, 0.5 cpd, 2 cpd, 4 cpd, and 8 cpd, respectively (Vimal, 1998, 2002; Webster et al., 1990).

The same controversy is also observed in visually evoked cortical potential (VECP) investigations. Many VECP studies have shown differences in the chromatic spatial selectivity (Arakawa, Tobimatsu, Tomoda, Kira, & Kato, 1999; Barboni et al., 2013; Berninger, Arden, Hogg, & Frumkes, 1989; Morrone, Burr, & Fiorentini, 1993; Porciatti & Sartucci, 1999; Rabin, Switkes, Crognale, Schneck, & Adams, 1994). Some of these studies have shown low-pass functions (Arakawa et al., 1999; Barboni et al., 2013; Berninger et al., 1989; Morrone et al., 1993) and other studies resulted in band-pass functions (Porciatti & Sartucci, 1999; Rabin et al., 1994).

Our group have investigated the visual cortical evoked potential generated by pseudorandom single stimulus presentation of chromatic and luminance contrast (Araújo, Souza, Gomes, & Silveira, 2013; Risuenho, Miquilini, Lacerda, Silveira, & Souza, 2015). Usually, pseudorandom stimuli have been used to allow multifocal recordings, and to provide spatial resolution to visual evaluation (Baseler, Sutter, Klein, & Carney, 1994). Moreover, several reports had shown that from pseudorandom VECP, it is possible to extract information from different visual mechanism present in the different slices of the kernels (Araújo et al., 2013; Baseler & Sutter, 1997; Gerth, Delahunt, Crognale, & Werner, 2003; Klistorner, Crewther, & Crewther, 1997; Risuenho et al., 2015). Our investigations using pseudorandom stimulation to evoke cortical activity have used a single stimulus to keep similar spatial features used to elicit conventional transient and steady-state VECPs, such as grating pattern (Gomes et al., 2010, 2006, 2008; Souza et al., 2008, 2013; Souza, Gomes, Saito, Silva-Filho, & Silveira, 2007).

Kernels represent the cross-correlated function between the visual activity recording and the numerical sequence derived from the m-sequence that modulated the stimulus (Sutter, 2001). Depending on the number of stimulus position on time, the kernels represent an approximation of the linear response to the stimulus (first order kernel) or a progressive system's deviation of the linearity (higher order kernels) (Muller & Meigen, 2016; Reid, Victor, & Shapley, 1997). The physiological meaning of each kernel and its slices is dependent on the type of stimulus presentation mode that is used, but they represent the interaction between the responses evoked by two stimuli associated to the binary values of the m-sequence (m-states) (Sutter, 2001). In our investigations, we recorded luminance and chromatic contrast modulated by a pseudorandom sequence and investigated the presence of contrast detection mechanism in the different slices of the kernels (Araújo et al., 2013; Risuenho et al., 2015). Risuenho et al. (2015) showed that in trichromats, the first slice of the second order kernel (K2.1) elicited by pattern reversal showed a positive deflection around 100 ms for the luminance stimulus and a later negative polarity for compound stimulus. Moreover, in dichromats, K2.1 had positive polarity for the luminance stimulus such as trichromats, but it was low or absent for the compound stimulus, indicating the chromatic dependence of this response.

In the current study, we extended the investigation of pseudorandom VECP elicited by compound stimulus to a wider range of SF to study the spatial selectivity of the visual cortex and determine if it is possible to associate these cortical responses with luminance or chromatic information contained in this stimulus.

2. Methods

2.1. Subjects

We evaluated 14 trichromatic volunteers and 16 volunteers with congenital color vision defects aged between 18 and 30 years (26.4 ± 7.5 years old) with normal or corrected visual acuity to 20/20 wearing refractive correction when was necessary. All volunteers were informed about the study and then signed the consent form. The procedures of the project were approved by the Ethics Committee in Research from Núcleo de Medicina Tropical, Universidade Federal of Pará (Protocol # 023/2011). For the color vision assessment of volunteers, we used the Colour Assessment and Diagnosis test (City University, London, UK).

2.2. Stimulus configuration

The stimulus was a horizontal grating occupying 8° of a square patch, generated by the VERIS Science system (version 6.9, ElectroDiagnostic-Imagging, EDI, San Mateo, CA), and displayed on a high spatial and temporal resolution 20″ CRT color monitor (75 Hz, 1200 pixels × 1240 pixels). All the participants viewed the stimulus passively at a viewing distance of 1 m. The stimulus was presented centrally with a 1° central fixation cross. We used eight spatial frequencies: 0.2, 0.4, 0.8, 2, 4, 6, 8, and 10 cpd. The minimum and maximum number of chromatic cycles was 1.6 and 80 cycles. The number of

luminance cycles was twice the number of chromatic cycles. In the present paper, we indicated the SF of the stimulus' chromatic component (half of the luminance contrast SF).

The gratings had compound contrast composed by luminance and red-green contrast (CIE1976 color space; red: u′ = 0.432, v′ = 0.527; green: u′ = 0.12, v′ = 0.564). The luminance Michelson contrast was 0.33, which was the maximum modulation obtained in the VERIS system for this kind of stimulus. The stimulus was modulated by a function resulting from the addition of two sinusoidal functions with half cycle rectification and phase lag of 180° (Eq. (1)). The waveforms for the red color (W_r) and for green color (W_g) equations are as follows:

$$W_r = (R_{max} sin(\theta f)/2) + dc$$
$$\begin{cases} if\ \ Wr > dc; \quad Wr = Wr \\ \quad else\ \ Wr = 0 \end{cases} \tag{1}$$

$$W_g = (-G_{max} sin(\theta f)/2) + dc$$
$$\begin{cases} if\ \ Wg \geq dc; \quad Wg = Wg \\ \quad else\ \ Wg = 0 \end{cases} \tag{2}$$

where R_{max} and G_{max} were the maximum luminance of the red and green colors, which were set to be equal (10 cd/m^2), f is SF, and dc is the base level of luminance (5 cd/m^2). Fig. 1 shows the luminance modulation, color modulation, and the visualization of the stimulus.

Stimuli were surrounded by a background with luminance kept at 10 cd/m^2 and the same mean chromaticity of the stimulus (CIE1976 color space: yellow: u′ = 0.276, v′ = 0.545). The luminance of the stimulus and background was measured using a colorimeter CS-100A (Minolta, Osaka, Japan). The stimulus used in this study was the same one used in Risuenho et al. (2015) (luminance contrast = 0.33) and similar to the one used in Lee et al. (2011) (luminance contrast = 1).

A binary m-sequence (2^{14}-1 elements) temporally controlled the stimulus presentation, and it was configured for pattern reversal mode. The base period of the m-sequence reading was 13.3 ms (Fig. 1). For each SF condition, the trial was composed of the recording of four segments (1 min, 4 sec each segment; 4 min, 16 sec each trial). No interval occurred between the segments. The SF stimulus conditions were randomly presented. The time duration between the trials was 1 min.

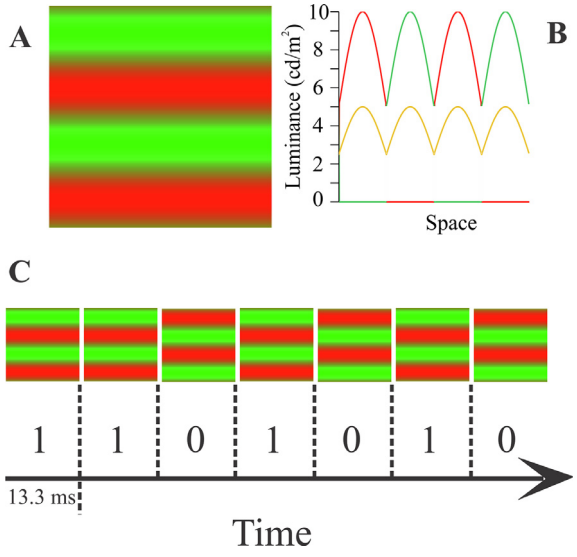

Fig. 1. Pseudo-random grating stimulus used in this work. *A*, horizontal red-green gratings were generated which were composed of luminance and red-green contrasts. *B*, color and luminance profiles across the vertical dimension of the grating stimulus: red and green curves show how the red and green lights varied, while the yellow curve shows how the mean luminance = (red + green)/2 varied across the stimulus vertical dimension. Both red luminance and green luminance were half-wave rectified sinusoidal functions while mean luminance varied as a full-wave rectified sinusoidal function. *C*, stimulus presentation along the time dimension was controlled by an m-sequence: 1 and 0 represent different stimulus spatial phase.

2.3. Recording settings

Gold surface electrodes were positioned according to the standards of the International Society of Clinical Electrophysiology of Vision (Odom et al., 2010). Active, inactive, and ground electrodes were placed at Oz, Fz, and Fpz points, respectively. The electroencephalogram was amplified 50,000 times, digitized at 1200 Hz, and Fourier filtered between 0.1 and 100 Hz. The electrode impedance was kept below 10 KΩ. The VERIS Science system (EDI, CA) was used to record the EEG and to extract the data of the kernels.

2.4. Analysis

An offline low-pass filter at 50 Hz was applied to the kernel waveforms. The amplitude of the VECP was measured from the peak to the baseline. Here, the baseline represents the average of the first 10 ms of each recording. For trichromats, all the VECP component amplitudes were normalized by the largest amplitude of each component from each participant. For each participant, each VECP component ranged between 0 and 1.

The SF response data were fitted by a difference of Gaussians function (Eq. (3)) by using the method of least squares with the Solver Add-in in Microsoft Excel. Previous studies have applied difference of two Gaussians to fit contrast sensitivity function (Enroth-Cugell & Robson, 1966, 1984).

The advantage of difference of Gaussians model to fit SF responses is that is possible to measure the SF spread that indicates the range of resolution of the neurons that contributed to the SF response functions (Shapley, 1993).

After the modelling of the SF response function, we extracted from the model the optimal SF, which was the SF with higher amplitude, and the bandwidth of SFs with an amplitude above ¾ of the maximum amplitude of the model. We expressed the bandwidth length in terms of octaves according to Eq. (4). Each individual model was classified as low-pass tuned when the amplitude of the model in the lower SF was above the ¾ of the model maximum amplitude as band-pass tuned when the amplitude of the model in the lower SF was below the ¾ of model maximum amplitude.

$$y = A \times e^{\left(-\frac{(x-\mu)^2}{2} \times c\right)} - B \times e^{\left(-\frac{(x-\rho)^2}{2} \times i\right)} \tag{3}$$

A and B are free parameters related to the amplitude of the Gaussian functions, μ and ρ are free parameters related to the mean of the Gaussian functions, c and i are standard deviations of the Gaussian functions.

$$y = \frac{\ln\left(\frac{SFhigh}{SFlow}\right)}{\ln(2)} \tag{4}$$

ln is the natural logarithm, *SFlow* is the lower SF with amplitude higher than ¾ of maximum amplitude of the model, *SFhigh* is the higher SF with amplitude higher than ¾ of maximum amplitude of the model.

The high SF cut-off was also estimated by the fit of a linear model to the amplitude data from the optimal SF to SF with an ideal zero amplitude. The fit was also obtained by using the method of least squares.

One-way repeated measures ANOVA was conducted to compare the high SF cut-off and the optimal SF obtained from the different VECP components. Tukey post hoc test was performed when necessary. For these analyses the significance level was adjusted for multiple comparisons (significance level = 0.05, number of multiple comparisons = 6, adjusted α = 0.05/6 = 0.0083). One-way repeated measures ANOVA was also conducted to compare the effect of SF on the VECP

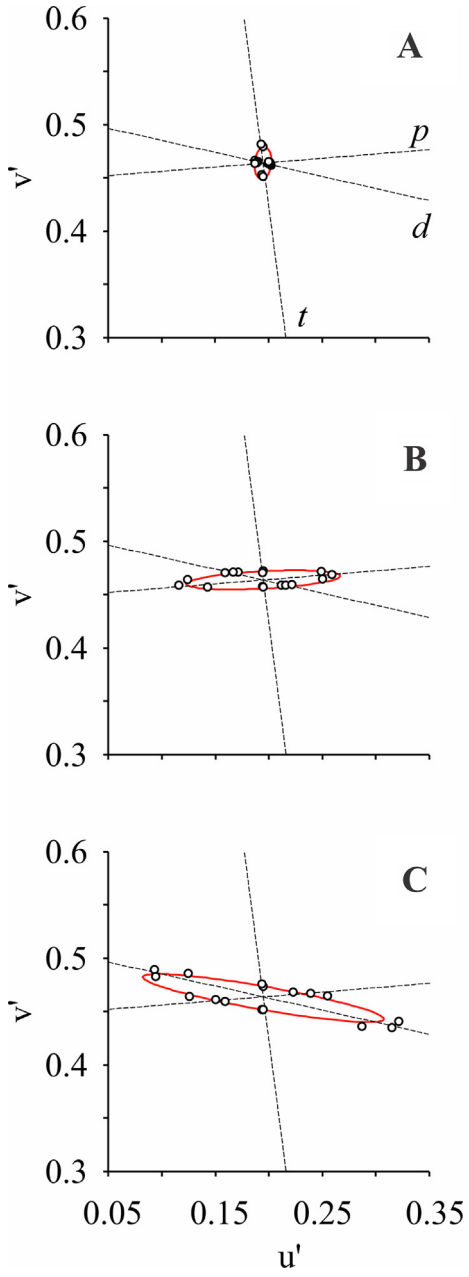

Fig. 2. Color discrimination ellipses of a trichromat (A), protanope (B), and deuteranope (C) in the CIE 1976 color diagram. White circles represent the color discrimination thresholds in 20 chromatic axes. Dashed lines represent the color confusion lines (*p*: protan, *d*: deutan, *t*: tritan).

component amplitude followed by Tukey post hoc test. For these analyses the significance level was adjusted for multiple comparisons (significance level = 0.05, number of multiple comparisons = 28, adjusted $\alpha = 0.05/28 = 0.0017$).

3. Results

3.1. Color vision phenotype

Color discrimination thresholds obtained from one representative trichromat, protanope and deuteranope are illustrated in the Fig. 2. The trichromats (n = 14) had smaller ellipses than the dichromats (5 protanopes and 11 deuteranopes), and the dichromats had the ellipse rotated to the protan or deutan confusion lines.

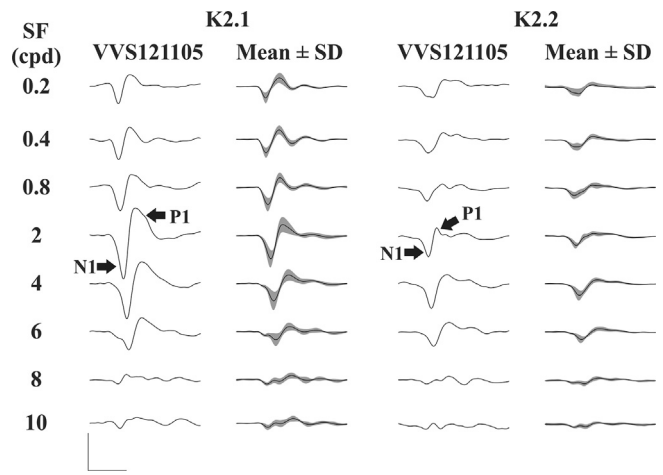

Fig. 3. Visual evoked cortical potential (VECP) waveforms obtained from normal trichromats. K2.1 and K2.2 VECP waveforms are displayed in the left and right pairs of columns, respectively. For both kernel slices, waveforms of a single individual are presented in the left column (VVS121105) while means and standard deviations (SD) for this subject group (n = 14) are presented in the right column (traces correspond to the mean values and shaded contours represent the standard deviations). In each column, from top to bottom, K2.1 and K2.2 VECP waveforms were obtained by using stimulus spatial frequencies (SF) of eight different values (0.2–10 cycles/degree). K2.1 waveforms had a negative component (N1 K2.1) followed by a positive component (P1 K2.1) in the interval 70–170 ms. K2.2 waveforms were dominated by a negative component in the interval 70–140 ms (N1 K2.2) followed by a small positive component (P1 K2.2) which was absent in some subjects. Scale bars: vertical = 10 μV, horizontal = 100 ms.

3.2. VECP waveforms

We identified that no signal was present in the first order kernel, but prominent cortical responses were observed in the first (K2.1) and second slices (K2.2) of the second order kernel. For trichromats, the mean waveforms of the K2.1 were characterized in the interval between 70 and 170 ms in the presence of a negative deflection (N1 K2.1) followed by a positive deflection (P1 K2.1) (Fig. 3). The mean waveforms of the K2.2 were dominated in the interval between 70 and 140 ms by a negative deflection (N1 K2.2) also followed by positive deflection (P1 K2.2) (Fig. 3).

Fig. 4 shows the K2.1 and K2.2 mean waveforms of protanopes. Similarly, Fig. 5 shows the same information for deuteranopes. In general, little or no response was found for the dichromats. In some subjects, we observed small positivity in the same latency of the N1 components seen in K2.1 and K2.2 for trichromats.

3.3. Effect of the spatial frequency on VECP components amplitude

Fig. 6 illustrated the modelling of the SF response function estimated from N1 K2.1 (Fig. 6A), P1 K2.1 (Fig. 6B), N1 K2.2 (Fig. 6C), and P1 K2.2 (Fig. 6D). For each VECP component, we compared the amplitude obtained at all SF we tested. For N1 K2.1, there was a significant effect of SF on the VECP amplitude ($F[2.334, 30.34] = 53.76$, $p < 0.0001$). For P1 K2.1, there was a significant effect of the SF on the VECP amplitude ($F[2.558, 33.25] = 8.484$, $p = 0.0005$). For N1 K2.2, there was a significant effect of SF on the VECP amplitude ($F[3.147, 40.91] = 20.83$, $p < 0.0001$). For P1 K2.2, the same again ($F[3.683, 47.88] = 5.642$, $p = 0.0011$). The results of the multiple VECP amplitude comparisons for each component are shown in the Fig. 7. We used a color coding to indicate the statistical outcomes: (i) the grey areas represent non-significant difference between the VECP amplitude obtained in the spatial frequencies indicated in the row and in the column; (ii) the green areas indicate a significant lower VECP amplitude

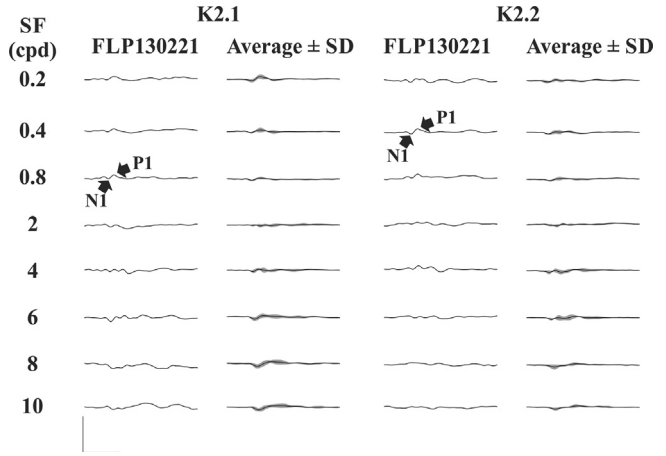

Fig. 4. VECP obtained from protans. Results for a single protan subject (CPV140611) and means and standard deviation for the protan group (n = 5). Figure structure and labels as in the previous Fig. 2. K2.1 and K2.2 waveforms showed residual cortical activity in red-green color-blind subjects between 100 and 150 ms, more often a very small negative component (N1) followed by a similar very small positive component (P1). Scale bars: vertical = 10 μV, horizontal = 100 ms.

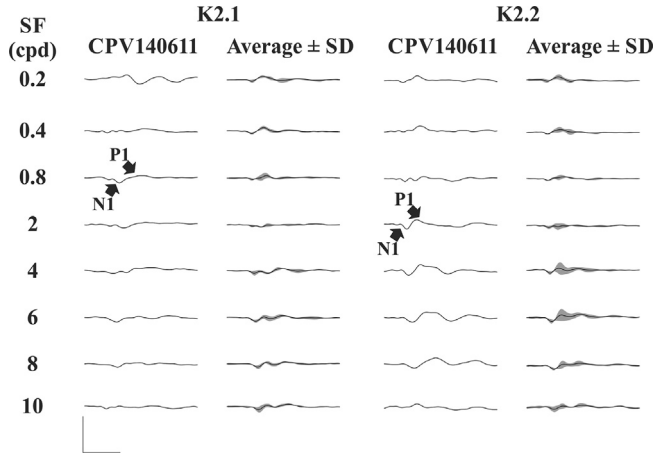

Fig. 5. VECP obtained from deutans. Results for a single deutan subject (FLP130221) and means and standard deviation for the deutan group (n = 11). Figure structure and labels as in the previous Fig. 2. Similarly to protans, cortical responses obtained from deutan subjects were also very small and featured a very small negative component (N1) followed by a very small positive component (P1). Responses from deutans were slightly smaller than responses obtained from protans. Scale bars: vertical = 10 μV, horizontal = 100 ms.

obtained at the SF indicated in the row than in that indicated in the column; (iii) the blue areas indicate a significant bigger VECP amplitude obtained at the SF in the row than that in the column. We observed that for negative components there was two significant areas. At low spatial frequencies (0.2–0.8 cpd) the VECP amplitudes were smaller than at the intermediate spatial frequencies (2–4 cpd), and at high spatial frequencies (especially 8–10 cpd) the VECP amplitude also were smaller than the intermediate and low spatial frequencies. We interpreted this finding as a band-pass profile of the SF response function. To the positive components, it was observed only the smaller VECP amplitude at the high spatial frequencies compared to the low and intermediate SF. We interpreted this finding as low-pass profile of the SF response function.

3.4. Comparisons of the spatial frequency response function parameters estimated from the different VECP components

Table 1 summarizes the optimal SF and band width for the SF response function estimated from the different VECP components. There was significant difference of the optimal SF obtained by the several pseudorandom VECPs components ($F[3,52] = 11.45$, $p < 0.0001$). N1 K2.1 component has significantly higher optimal SF than P1 K2.1, but not than N1 and P1 K2.2. P1 K2.1 optimal SF also was significantly smaller than the optimal SF obtained in N1 and P1 K2.2. No difference was found between the optimal frequency estimated by N1 and P1 K2.2 database. No difference was found comparing the bandwidth estimated from the functions obtained of the negative components. There was significant difference of the high frequency cut-off obtained by the several pseudorandom VECPs components ($F[3,52] = 4.049$, $p = 0.011$). The multiple comparison showed that there was one significant difference between two VECP components, which was between N1 and P1 K2.1.

In order to estimate the possible responses for dichromat subjects, we considered the highest negativity and positivity between 70 and 140 ms in the K2.1 at all spatial frequencies. Fig. 8 shows the comparison between the SF response function estimated of the K2.1 and K2.2 information from trichromats and each dichromat group.

4. Discussion

The goal of the present study was to evaluate the SF response function for a visual evoked potential generated by a compound stimulus modulated by m-sequences. The present study is the first description of spatial selectivity estimated by using pseudo-random VECP elicited by a stimulus composed of luminance and chromatic contrasts. Even though the stimulus we used has color and luminance contrast, the cortical response we obtained seems to be dominated by the contribution of chromatic-sensitive mechanism. Three findings encouraged us to suggest that our data represent mechanisms of cortical processing for color information: (i) The first finding was the absence of responses in subjects with congenital color vision deficiencies; (ii) The second finding was that the high SF cut-offs estimated from the several VECP components resembled the visual acuity obtained for chromatic stimulation in psychophysics experiments with humans (Mullen, 1985); (iii) The third finding was the presence of multiple SF tuning mechanisms similar to those shown by color-sensitive cortical cells in V1 (Johnson et al., 2001).

4.1. Absence of responses in subjects with congenital color vision deficiencies

We tested subjects with congenital deficiency for red-green color vision as negative controls. The results obtained from those volunteers showed small positive-dominated responses for the compound stimulus response, indicating some contribution from luminance mechanisms such as found in Risuenho et al. (2015) and Gomes et al. (2006). We used luminance contrast of 33% in the compound stimulus to generate the VECPs. Araújo et al. (2013) observed very reliable pseudorandom VECPs for achromatic stimulus with similar luminance contrast (25%) at 0.4, 2 and 10 cpd. It is also suggested that to record color-opponent cortical responses to red-green gratings, the stimulus should contain up to 8–12 spatial cycles to avoid luminance intrusions (chromatic aberration) on the isoluminant chromatic stimulus (Kulikowski, Robson, & McKeefry, 1996). We used spatial frequencies with much more spatial cycles than the recommendations. In the present work, small negative and positive peaks are actually observed in K2.1 and K2.2 from dichromats as shown in Figs. 4 and 5. These responses could be hypothesized to be responses to luminance component of the compound stimuli or response to the luminance artifact of the chromatic component of the compound stimulus. We are introducing real luminance

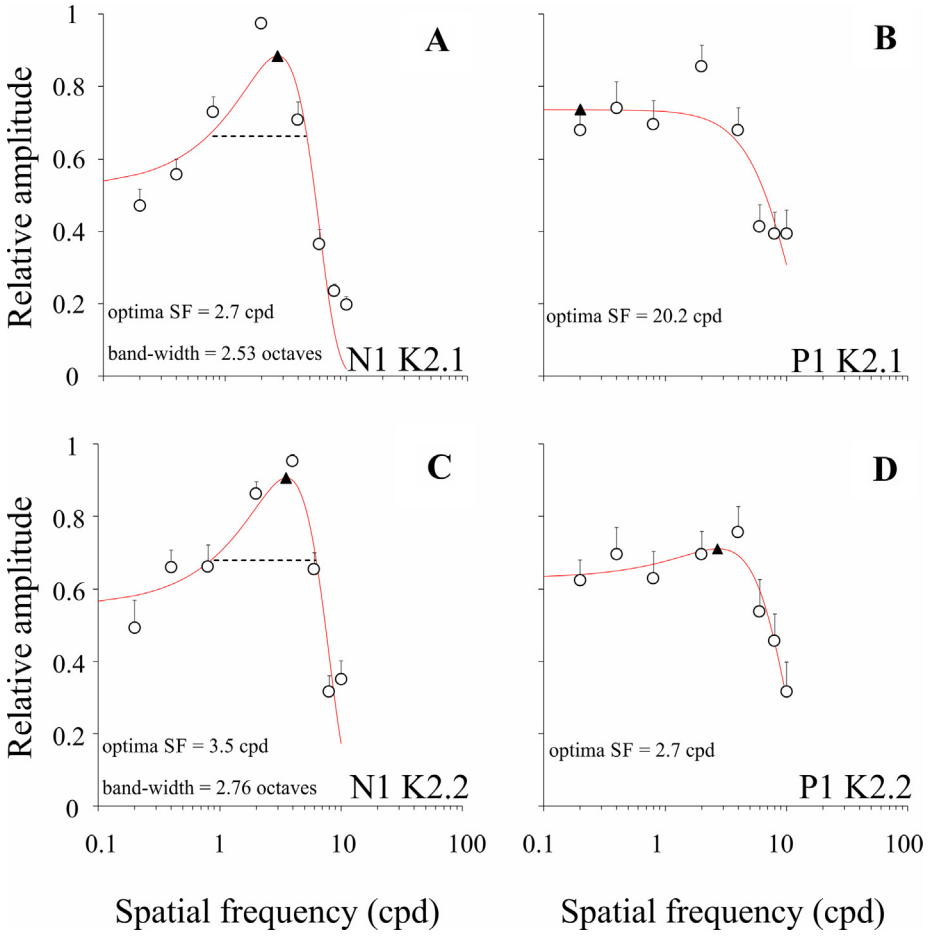

Fig. 6. VECP amplitude as a function of spatial frequency for normal trichromats A-D, relative amplitude of different VECP components (circles) as a function of spatial frequency fitted with DoG (difference of Gaussian) functions (red curves). N1 K2.1 (A) and N1 K2.2 (C) components show a band-pass function peaking at 2–4 cycles/degree with very little response at low spatial frequencies. P1 K2.1 (C) and P1 K2.2 (D) components show a low-pass function with very little attenuation at spatial frequencies lower than 2–4 cycles/degree. SF: spatial frequency, cpd: cycles/degree. Circles and bars represent means and standard errors (sample size = 14). Black triangle represents the optimal SF. Horizontal dashed line represents the bandwidth range.

contrast that probably mask the luminance artifact that could be considered a positive thing compared to isoluminant chromatic grating, specially at high SF range. In the present study, VECP amplitude from dichromats for the luminance component of the compound stimulus (33% of contrast) was very small compared to the pseudorandom VECP amplitude observed by Araújo et al. (2013) that recorded pseudorandom VECP elicited by isochromatic luminance spatial contrast gratings.

4.2. High spatial frequency cut-offs estimated from the several VECP components resembled the visual acuity obtained for chromatic stimulation in psychophysics experiments with humans

The high SF cut-offs estimated in the present study also corroborated our hypothesis that the pseudorandom VECP elicited by the compound stimulus actually activated color opponent pathways. We found high SF cut-off between 10 and 15 cpd, whose were near those found psychophysically by Mullen (1985) at 11 or 12 cpd.

We found that trichromats had N1 K2.1 and N1 K2.2 amplitudes as a function of SF with band-pass tuning. Moreover, P1 K2.1 and P1 K2.2 amplitude showed low-pass tuning across the SF domain. Several studies have used VECP as a tool to explain the spatial selectivity of color vision (Arakawa et al., 1999; Barboni et al., 2013; Berninger et al., 1989; Morrone et al., 1993; Porciatti & Sartucci, 1999; Rabin et al., 1994). The present data show some similarities and differences from previous studies. The differences probably occurred due to factors such as the temporal frequency of the stimulus, the presentation mode, and the perceptual level of the estimated response.

According to the temporal frequency, conventional VECP can be classified as transient or steady-state (for review see in Tobimatsu & Celesia, 2006). In the present study, pseudorandom VECPs were generated by stimulation modulated by m-sequence step duration of 13.3 ms, which is in the steady-state temporal frequency range. Pseudorandom VECP components had different SF tuning (negative components: band-pass tuning; positive components: low-pass tuning), while steady-state VECP SF tuning have been described as low-pass profile (Arakawa et al., 1999; Barboni et al., 2013; Morrone et al., 1993), and transient VECPs have shown primarily band-pass tuned functions (Berninger et al., 1989; Porciatti & Sartucci, 1999; Rabin et al., 1994). Our results do not clarify the direct relationship that pseudorandom VECPs and steady-state VECPs could share because of the similarities in the temporal frequency features of the stimuli.

Mckeefry, Russell, Murray, and Kulikowski (1996) reported that chromatic onset-offset VECP activated mechanisms of sustained responses and the chromatic pattern reversal VECPs would activate mechanisms with transient characteristics. Studies that used the onset-offset presentation mode described SF response functions with band-pass profile (Berninger et al., 1989; Porciatti & Sartucci, 1999; Rabin et al., 1994), while studies, using the pattern reversal described SF response functions with low-pass tuning (Arakawa et al., 1999; Barboni et al., 2013; Berninger et al., 1989; Morrone et al., 1993). Using conventional VECP has shown that onset presentation mode preferentially separated the chromatic and luminance mechanisms because the cortical response had opposite polarity for each mechanism (Carden, Kulikowski, Murray, & Parry, 1985). In the present study, we used pattern reversal configuration to elicit the pseudorandom VECPs following our findings in Risuenho et al. (2015), which showed inverted polarities to luminance and chromatic cortical responses in the K2.1, while onset presentation elicited deflections with same polarity (Risuenho et al., 2015). It is not clear how to reconcile the transient and sustained mechanisms described for transient VECP and the kernels of the pseudorandom VECPs. The theoretical interpretation of the kernel

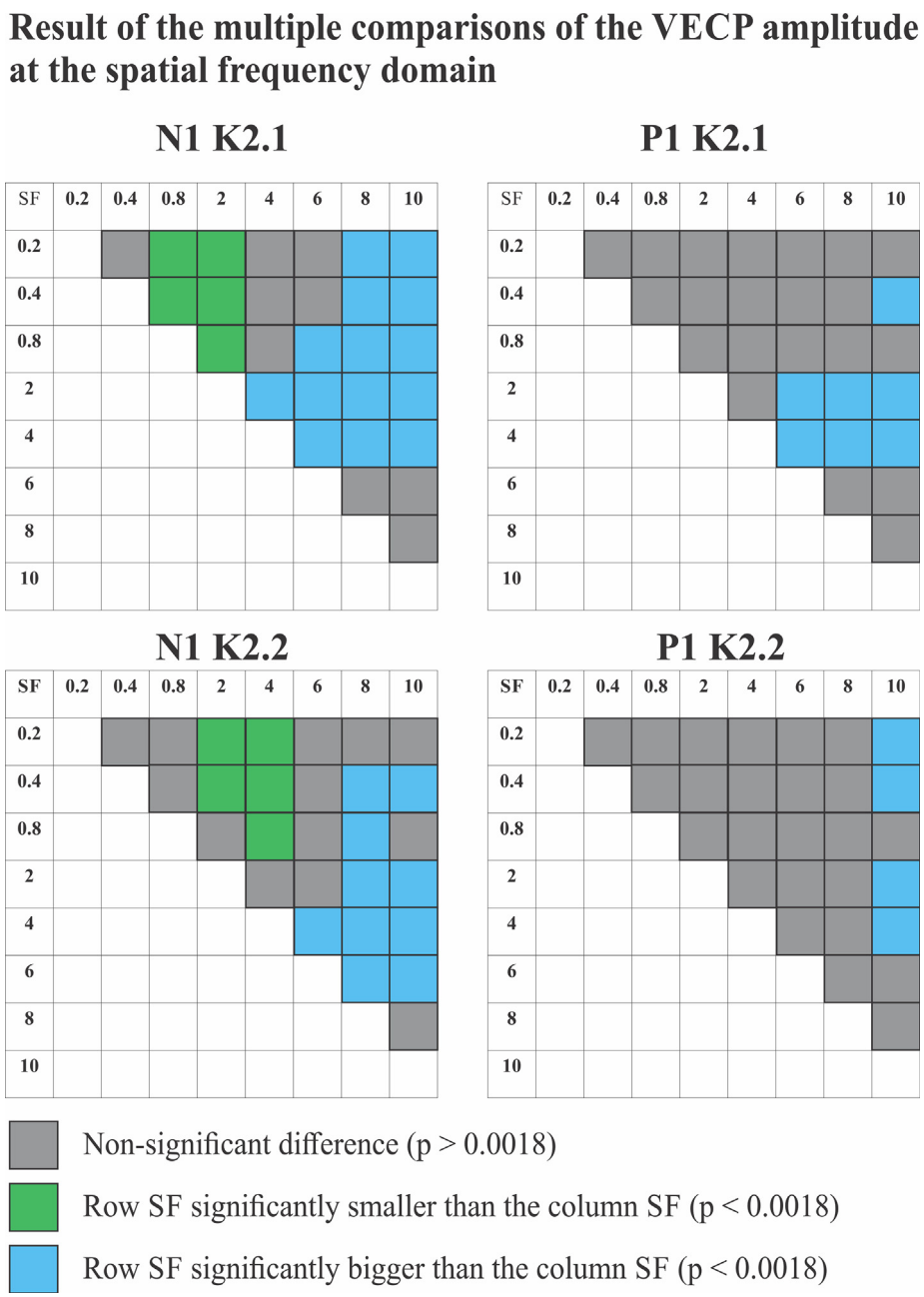

Fig. 7. Tile plots of the VECP amplitude multiple comparisons among different spatial frequencies for N1 K2.1 (A), P1 K2.1 (B), N1 K2.2 (C), P2 K2.2 (D). Gray tiles represent non-significant difference in the comparison ($p > 0.05$); Green tiles represent that the VECP amplitude elicited by the spatial frequency indicated in the row was significantly smaller than that elicited by the spatial frequency indicated in the column; Blue tiles represent that the VECP amplitude elicited by the spatial frequency indicated in the row was significantly bigger than that elicited by the spatial frequency indicated in the column. SF: spatial frequency.

Table 1
Summary of the spatial frequency selectivity parameters of the VECP components.

VECP component	Optimal frequency (cpd)	Bandwidth (octaves)	High frequency cut-off (cpd)
N1 K2.1	2.4 ± 1	2.86 ± 1.6	10.4 ± 1.7
P1 K2.1	0.7 ± 1.5	–	13.8 ± 3.6
N1 K2.2	3.5 ± 0.7	2.89 ± 1.5	11.5 ± 0.8
P1 K2.2	2.54 ± 1.7	–	12.6 ± 3.6

slices (Sutter, 2000), K2.1 components represent the interaction of visual responses separated by shorter time interval than the K2.2 components, indicating the K2.1 could be better candidate to reflect the transient mechanisms of the visual system than K2.2 that could be interpreted as an indicator of sustained mechanism of contrast detection.

4.3. Presence of multiple spatial frequency tuning mechanism

Araújo et al. (2013) suggested the existence of multiple mechanisms for luminance SF and contrast detection of pseudorandom single gratings. K2.1 waveform was dominated by positive component that had low-pass SF tuning and K2.2 waveform was dominated by a negative component that had band-pass SF tuning and peaked at 2–4 cpd. In the present paper, we described that using compound stimuli, we continue observing multiple mechanisms to describe the SF selectivity of the second-order kernel. The recording of the activity from different group of cells in V1 have demonstrated at least three profiles of spatial

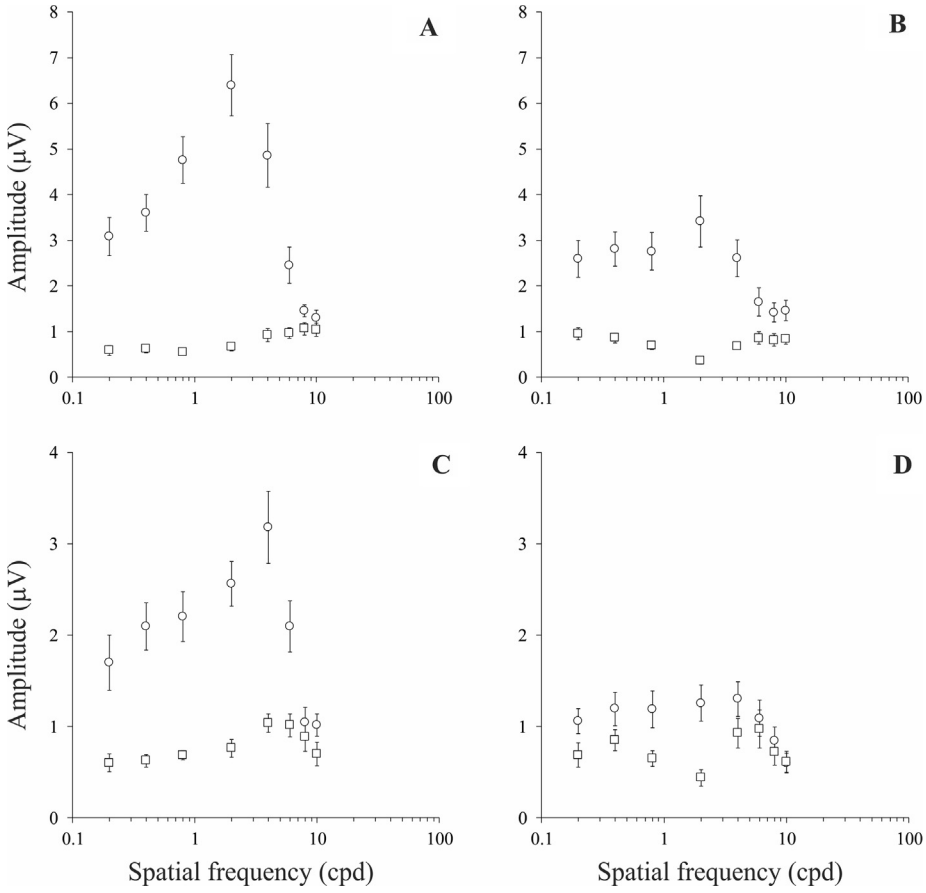

Fig. 8. Spatial frequency response for trichromats, protans, and deutans Comparison between the mean spatial frequency response functions obtained from K2.1 VECP recorded from trichromats (circles), and dichromats (squares). Symbols and bars represent means and standard error. A, N1 K2.1. B, P1 K2.1. VECP responses obtained from colorblind subjects (protanopes and deuteranopes) are small, very often in the limit of noise.

selectivity (Johnson et al., 2001; Li et al., 2014): band-pass profile for luminance sensitive-cells; band-pass profile for color-luminance sensitive cells; and low-pass profile for color sensitive cells. We found band-pass and low-pass functions for different components of the first and second slices of the second order kernel: negative components had band-pass profile, and positive components had low-pass profile. The association between the cortical neurons with different SF-response profiles and our pseudo-random VECP components would be speculative.

However we have found similarities between optimal SF, and bandwidth obtained from N1 K2.1 and N1 K2.2 components and those estimated in V1 cells responsive to color-luminance stimulus, as well as the same parameters obtained from P1 K2.1 and P1 K2.2 components and those estimated from neurons that respond exclusively or preferentially for equiluminant chromatic stimuli. Hood et al. (2006) compared contrast-mfVECP response functions to a model of V1 activity and observed that the model described well the mfVECP amplitude up to 40% of luminance contrast. At high luminance contrast level, mfVECP differed from the V1 activity model and led the authors to suggest that mfVECP is not entirely generated from V1, and extra-striatal neuros probably contributes to the mfVECP generation. A possible reason to explain the partial adjustment of the contrast-mfVECP response function to the V1 model is that the stimulus used by Hood et al. (2006) was very large (23° field) and the V1 model was estimated using neurons responding for a central 5° field, and the pseudorandom responses would receive contribution of neurons with different contrast sensitivity located in different visual eccentricities. Later, Laron, Cheng, Zhang, and Frishman (2009) demonstrated that the contrast response function estimated for the stimulation of the central vision had lower gain compared to that estimated from the stimulation of the more peripheral visual field sectors. They also demonstrated that the contrast-response functions for central fields were closer to the V1 model than the functions which received contribution from central and peripheral fields. As we used an 8° stimulus, more than 5° central field expected for V1 activity, we considered that our results reflect mainly the activation of V1, but as it is reasonable that extra-striatal areas also contribute to the pseudorandom VECPs we obtained.

We concluded that pseudorandom VECP elicited by compound stimulus was dominated by chromatic detection mechanism, and that different components of the first and second slices of the second order kernel could reflect the activity of two different cortical color mechanisms could be activated. New investigations are necessary to bring more information about the functional role of joint processing of color and luminance and of the isolated processing of color or luminance information.

Author contributions

LCLS, GSS contributed in the conception and design of the experiments, revised critically the manuscript for important intellectual content. LM, AB contributed in the data analysis, and drafted the manuscript. PRKG and AMH drafted the manuscript. ICVSM collected, analysed and interpreted the database.

Declaration of Competing Interest

The authors declare that they have no known competing financial interests or personal relationships that could have appeared to influence the work reported in this paper.

Acknowledgments

This research was supported by the following grants: CNPq # 431748/2016-0; CNPq-PRONEX/FAPESPA #316799/2009; and FINEP

IBN Net #1723. ICVSM received CAPES fellowship for graduate students. LCLS, GSS, and AMH are CNPq research fellows.

Appendix A. Supplementary data

Supplementary data to this article can be found online at https://doi.org/10.1016/j.visres.2019.09.004.

References

Arakawa, K., Tobimatsu, S., Tomoda, H., Kira, J., & Kato, M. (1999). The effect of spatial frequency on chromatic and achromatic steady-state visual evoked potentials. *Clinical Neurophysiology, 110*, 1959–1964.

Araújo, C. S., Souza, G. S., Gomes, B. D., & Silveira, L. C. L. (2013). Visual evoked cortical potential (VECP) elicited by sinusoidal gratings controlled by pseudo-random stimulation. *PLoS ONE, 8*, e70207.

Barboni, M. T. S., Gomes, B. D., Souza, G. S., Rodrigues, A. R., Ventura, D. F., & Silveira, L. C. L. (2013). Chromatic spatial contrast sensitivity estimated by visual evoked cortical potential and psychophysics. *Brazilian Journal of Medical and Biological Research, 46*, 154–163.

Baseler, H. A., & Sutter, E. E. (1997). M and P components of the VEP and their visual field distribution. *Vision Research, 37*, 675–690.

Baseler, H. A., Sutter, E. E., Klein, S. A., & Carney, T. (1994). The topography of visual evoked response properties across the visual field. *Electroencephalography and Clinical Neurophysiology, 90*, 65–81.

Berninger, T. A., Arden, G. B., Hogg, C. R., & Frumkes, T. (1989). Colour vision defect diagnosed by evoked potentials. *Investigative Ophthalmology & Visual Science, 30*, 290–299.

Carden, D., Kulikowski, J. J., Murray, I. J., & Parry, N. R. A. (1985). Human occipital potentials evoked by the onset of equiluminant chromatic gratings. *Journal of Physiology (London), 369*, 44P.

Cooper, B., Sun, H., & Lee, B. B. (2012). Psychophysical and physiological responses to gratings with luminance and chromatic components of different spatial frequencies. *Journal of the Optical Society of America A Optics, Image Science, and Vision, 29*, 314–323.

Dow, B. M. (1974). Functional classes of cells and their laminar distribution in monkey visual cortex. *Journal of Physiology, 37*, 927–946.

Enroth-Cugell, C., & Robson, J. G. (1966). The contrast sensitivity of retinal ganglion cells of the cat. *Journal of Physiology, 187*, 517–552.

Enroth-Cugell, C., & Robson, J. G. (1984). Functional characteristics and diversity of cat retinal ganglion cells. *Investigative Ophthalmology & Visual Science, 25*, 250–267.

Gerth, C., Delahunt, P. B., Crognale, M. A., & Werner, J. S. (2003). Topography of the chromatic pattern-onset VEP. *Journal of Vision, 3*, 171–182.

Gomes, B. D., Souza, G. S., Rodrigues, A. R., Saito, C. A., Silveira, L. C., & da Silva Filho, M. (2006). Normal and dichromatic color discrimination measured with transient visual evoked potential. *Visual Neuroscience, 23*, 617–627.

Gomes, B. D., Souza, G. S., Saito, C. A., Silva-Filho, M., Rodrigues, A. R., & Silveira, L. C. L. (2010). *Ophthalmic and Physiological Optics, 30*, 518–524.

Hood, D. C., Ghadiali, Q., Zhang, J. C., Graham, N. V., Wolfson, S., & Zhang, X. (2006). Contrast-response functions for multifocal visual evoked potentials: A test of a model relating V1 activity to multifocal visual evoked potentials activity. *Journal of Vision, 6*, 4. https://doi.org/10.1167/6.5.4.

Hubel, D. H., & Wiesel, T. N. (1968). Receptive fields and functional architecture of monkey striate cortex. *Journal of Physiology, 195*(215–243), 1968.

Johnson, E. N., Hawken, M. J., & Shapley, R. (2001). The spatial transformation of colour in the primary visual cortex of the macaque monkey. *Nature, 4*, 409–416.

Klistorner, A., Crewther, D. P., & Crewther, S. G. (1997). Separate magnocellular and parvocellular contributions from temporal analysis of the multifocal VEP. *Vision Research, 37*, 2161–2216.

Kulikowski, J. J., Robson, A. G., & McKeefry, D. J. (1996). Specificity and selectivity of chromatic visual evoked potentials. *Vision Research, 36*, 3397–3401.

Laron, M., Cheng, H., Zhang, B., & Frishman, L. (2009). The effect of eccentricity on the contrast response function of multifocal visual evoked potentials (mfVEPs). *Vision Research, 49*, 1711–1716.

Lee, B. B., Sun, H., & Valberg, A. (2011). Segregation of chromatic and luminance signals using a novel grating stimulus. *Journal of Physiology, 589*, 59–73.

Lennie, P., Krauskopf, J., & Sclar, G. (1990). Chromatic mechanisms in striate cortex of macaque. *Journal of Neuroscience, 10*, 649–669.

Li, X., Chen, Y., Lashgari, R., Bereshpolova, Y., Swadlow, H. A., Lee, B. B., & Alonso, M. (2014). Mixing of chromatic and luminance retinal signal in primate area V1. *Cerebral Cortex*. https://doi.org/10.1093/cercor/bhu002.

Mckeefry, D. J., Russell, M. H. A., Murray, I. J., & Kulikowski, J. J. (1996). Amplitude and phase variations of harmonic components in human achromatic and chromatic VEPs. *Visual Neuroscience, 13*, 639–653.

Morrone, M. C., Burr, D. C., & Fiorentini, A. (1993). Development of infant contrast sensitivity to chromatic stimuli. *Vision Research, 33*, 2535–2552.

Mullen, K. T. (1985). The contrast sensitivity of human colour vision to red-green and blue-yellow chromatic gratings. *Journal of Physiology, 359*, 381–400.

Muller, P. L., & Meigen, T. (2016). M-sequences in ophthalmic electrophysiology. *Journal of Vision, 16*, 15.

Odom, J. V., Bach, M., Brigell, M., Holder, G. E., McCulloch, D. L., Tormene, A. P., et al. (2010). ISCEV standard for clinical visual evoked potentials (2009 update). *Documenta Ophthalmologica, 120*, 111–119.

Parry, N. R., Murray, I. J., Panorgias, A., Mckeefry, D. J., Lee, B. B., & Kremers, J. J. (2012). Simultaneous chromatic and luminance human electroretinogram responses. *Journal of Physiology, 590*, 3141–3154.

Porciatti, V., & Sartucci, F. (1999). Normative data for onset VEPs to red-green and blue-yellow chromatic contrast. *Clinical Neurophysiology, 110*, 772–781.

Rabin, J., Switkes, E., Crognale, M., Schneck, M. E., & Adams, A. J. (1994). Visual evoked potentials in three-dimensional colour space: Correlates of spatio-chromatic processing. *Vision Research, 34*, 2657–2671.

Reid, R. C., Victor, J. D., & Shapley, R. M. (1997). The use of m-sequences in the analysis of visual neurons: Linear receptive field properties. *Visual Neuroscience, 14*, 1015–1027.

Risuenho, B. B. O., Miquilini, L., Lacerda, E. M. C. B., Silveira, L. C. L., & Souza, G. S. (2015). Cortical responses elicited by luminance and compound stimuli modulated by pseudo-random sequences: Comparison between normal trichromats and congenital red-green colour blinds. *Frontiers in Psychology, 6*. https://doi.org/10.3389/fpsyg.2015.00053.

Shapley, R. (1993). Introduction. Contrast sensitivity. Shapley, R & Lam, DM-K. Cambridge: MIT press, xi-xx.

Souza, G. S., Gomes, B. D., Lacerda, E. M. C. B., Saito, C. A., Silva-Filho, M., & Silveira, L. C. L. (2008). Amplitude of the transient visual evoked potential (tVEP) as function of achromatic and chromatic contrast: Contribution of different visual pathways. *Visual Neuroscience, 25*, 317–325.

Souza, G. S., Gomes, B. D., Lacerda, E. M. C. B., Saito, C. A., Silva-Filho, M., & Silveira, L. C. L. (2013). Contrast sensitivity of pattern transient VEP components: Contribution from M and P pathways. *Psychology & Neuroscience, 6*, 191–198.

Souza, G. S., Gomes, B. D., Saito, C. A., Silva-Filho, M., & Silveira, L. C. L. (2007). Spatial luminance contrast sensitivity measured with transient VEP: Comparison with psychophysics and evidence of multiple mechanisms. *Investigative Ophthalmology & Visual Science, 48*, 3396–3404.

Sutter, E. E. (2000). The interpretation of multifocal binary kernels. *Documenta Ophthalmologica, 100*, 49–75.

Sutter, E. E. (2001). Imaging visual function with the multifocal m-sequence technique. *Vision Research, 41*, 1241–1255.

Thorell, L. G., De Valois, R. L., & Albrech, D. G. (1984). Spatial mapping of monkey V1 cells with pure colour and luminance stimuli. *Vision Research, 24*, 751–769.

Tobimatsu, S., & Celesia, G. G. (2006). Studies of human visual pathophysiology with visual evoked potentials. *Clinical Neurophysiology, 117*, 1414–1433.

Vimal, R. P. (1998). Spatial-frequency tuning of sustained nonoriented units of the red-green channel. *Journal of the Optical Society of America A Optics, Image Science, and Vision, 15*, 1–15.

Vimal, R. P. (2002). Spatial-frequency-tuned mechanisms of the red-green channel estimated by oblique masking. *Journal of the Optical Society of America A Optics, Image Science, and Vision, 19*, 276–288.

Webster, M. A., De Valois, K. K., & Switkes, E. (1990). Orientation and spatial-frequency discrimination for luminance and chromatic gratings. *Journal of the Optical Society of America A Optics, Image Science, and Vision, 7*, 1034–1049.